Solar Energy Materials & Solar Cells 117 (2013) 429–436

Contents lists available at SciVerse ScienceDirect

Solar Energy Materials & Solar Cells

journal homepage: www.elsevier.com/locate/solmat

An artificial vasculature for adaptive thermal control of windows

Benjamin D. Hatton [a,b,1], Ian Wheeldon [a,2], Matthew J. Hancock [d], Mathias Kolle [a,b], Joanna Aizenberg [a,b], Donald E. Ingber [a,b,c,*]

[a] Wyss Institute for Biologically Inspired Engineering at Harvard University, Boston, MA 02115, USA
[b] School of Engineering and Applied Sciences, Harvard University, Cambridge, MA 02138, USA
[c] Vascular Biology Program, Departments of Pathology & Surgery, Boston Children's Hospital and Harvard Medical School, Boston, MA 02115, USA
[d] Broad Institute, Cambridge, MA, 02141, USA

ARTICLE INFO

Article history:
Received 15 February 2013
Received in revised form
4 June 2013
Accepted 17 June 2013

Keywords:
Convective cooling
Heat transfer
Microfluidic
Optical absorption
Window

ABSTRACT

Windows are a major source of energy inefficiency in buildings. In addition, heating by thermal radiation reduces the efficiency of photovoltaic panels. To help reduce heating by solar absorption in both of these cases, we developed a thin, transparent, bio-inspired, convective cooling layer for building windows and solar panels that contains microvasculature with millimeter-scale, fluid-filled channels. The thin cooling layer is composed of optically clear silicone rubber with microchannels fabricated using microfluidic engineering principles. Infrared imaging was used to measure cooling rates as a function of flow rate and water temperature. In these experiments, flowing room temperature water at 2 mL/min reduced the average temperature of a model 10×10 cm^2 window by approximately 7–9 °C. An analytic steady-state heat transfer model was developed to augment the experiments and make more general estimates as functions of window size, channel geometry, flow rate, and water temperature. Thin cooling layers may be added to one or more panes in multi-pane windows or as thin film non-structural central layers. Lastly, the color, optical transparency and aesthetics of the windows could be modulated by flowing different fluids that differ in their scattering or absorption properties.

1. Introduction

A significant amount of thermal energy is transferred through building windows, both in the summer (heat gain) and winter (heat loss). In fact, windows typically represent the most significant factor responsible for building energy inefficiencies, due to this thermal loss or gain. Recent estimates suggest that windows account for about 40% of total building energy costs [1]. Yet windows are obviously a necessary feature of architecture, and in fact, architectural trends seem to show increasing usage of glass in building facades, which intensifies the problem further. Advanced fenestration systems have thus been developed to improve building efficiency, thermal comfort, and cost effectiveness [2–8]. Multi-pane windows, reflective glazing, low-emissivity (low-e) coatings, and variable tint are all technologies that have improved window and building efficiency [2–8]. Thin plastic films have been proposed as non-structural center panes to increase efficiency while maintaining overall window width, mass, and visual transmittance [9]. Flowing air or water between double panes was recently proposed to cool window panes and prevent window heat from being conducted to the building interior [10,11]. The design included air or water that naturally flowed upward due to buoyancy, or air/water pumped upward at higher speeds [10,11]. Since the thermal conductivity of water is much higher than that of air, the efficiencies of the water cooled designs were estimated to be higher [10,11].

In addition to building fenestration, semiconductor photovoltaic (PV) solar panels can suffer from absorptive heating, which reduces their energy generating efficiency by approximately 5% for each degree increase in operating temperature over 50 °C [12–14]. In fact, there are designs of hybrid photovoltaic–thermal (PV/T) solar collectors that collect thermal energy by convective cooling, generally using a series of pipes filled with flowing water behind the PV panels [15,16]. Therefore, cooling mechanisms for building windows can also benefit solar panel design.

In contrast to man-made thermal control systems, living organisms have evolved an entirely different and highly efficient mechanism to control temperature that is based on the design of internal vascular networks. For example, blood vessels dilate to increase blood flow close to the skin surface to increase convective

* Corresponding author at: Wyss Institute for Biologically Inspired Engineering at Harvard University, Boston, MA 02115, USA.
E-mail address: don.ingber@wyss.harvard.edu (D.E. Ingber).
[1] Current address: Department of Materials Science and Engineering, University of Toronto, Toronto, ON M5S3E4, Canada.
[2] Current address: Department of Chemical and Environmental Engineering, University of California, Riverside, CA 92521, USA.

0927-0248/$ - see front matter © 2013 Elsevier B.V. All rights reserved.
http://dx.doi.org/10.1016/j.solmat.2013.06.027

heat transfer, whereas they constrict and limit flow when our skin is exposed to cold. In some birds, such as penguins, a counter-current flow mechanism is utilized within the vasculature to efficiently maintain a minimum temperature in the extremities [17]. Here we describe a new bio-inspired approach to thermal control for cooling (or heating) building window surfaces by incorporating transparent microfluidic heat exchange layers. The same approach may be used to control heat transfer across solar panel surfaces and improve the overall energy efficiency by reducing the operating temperature. Our results show that an artificial vascular network within a transparent layer, composed of channels on the micrometer to millimeter scale, and extending over the surface of a window, offers an additional and novel cooling mechanism for building windows and a new thermal control tool for building design.

2. Results

2.1. Temperature control in microfluidic windows

Experiments were conducted to explore the extent that an artificial vascular network lining a window surface can efficiently control the window temperature (or equivalently, the heat transfer across the window). We adapted microfluidic engineering techniques to fabricate optically clear, flexible elastomer sheets, containing rectangular channels, which were bonded to a glass window pane. Though single pane windows were used in our experiments for proof of concept, adding similar vasculature layers to one or more panes in a multi-pane window or engineering thin film non-structural central layers with vasculature are straightforward. The thin elastomer sheets were polydimethylsiloxane (PDMS) with channels having rectangular cross sections. Our two designs, called Diamond 1 and Diamond 2, had channel cross-sections (width by height) of 1 mm by 0.10 mm and 2 mm by 0.10 mm, respectively. The channels lined one side of the PDMS so that sealed networks of rectangular channels were formed when the PDMS layers were bonded to glass sheets (1/8″ thick, Fig. 1A). Flow entered an inlet on one side of a window and was distributed through a diamond network of channels (Fig. 1B). Importantly, although the channels were visible prior to infusion of liquid, they were not clearly visible when the channels were filled with water (Fig. 1B). The channels became almost entirely invisible if perfused with a fluid that more closely matched the refractive index of PDMS (1.43, data not shown).

Thermal infrared (IR) imaging enabled the thermal heat distribution of microvasculature networks to be visualized as a function of channel size, flow rate and initial water temperature. Prior to initiating fluid flow, the PDMS-glass composite window was heated by an incandescent light source (50 cm from the glass) to an initial temperature ranging from 35 to 40 °C. Water maintained at room temperature (RT, 21 °C) was then pumped through the microvascular channels at flow rates of 0.20, 2.0 and 10 mL/min. Changes in surface temperature were visualized using an IR camera as a function of the flow rate (Fig. 2A; darker colors indicate lower temperatures). The lowest flow rate (0.20 mL/min) had little effect on the overall window temperature, except around the inlet, while the high flow rate (10 mL/min) uniformly cooled the entire channel region whether the water flowing from the inlet was maintained at RT (Fig. 5) or 0 °C (Figs. 2, 5). Also, while the individual channels were initially visible, the cooled region spread to cover the entire microchannel network, reaching steady state within about 5 min for all flow rates.

To quantify the cooling effect, the window temperatures were averaged along a line extending between the inlet and outlet ports. This average window temperature was measured as a function of time for our Diamond 1 and 2 model windows described above at different flow rates (0.2, 2.0 and 10 mL/min). When the flow rate was higher than 0.20 mL/min, there was a significant drop in the average window temperature when water flowed through the channels at either 0 °C (Fig. 3A) or RT (Fig. 3B). As expected, the 0 °C flow at 10 mL/min caused the greatest cooling (to 8 °C, from the initial 35 °C), but even a modest flow of 2.0 mL/min of RT water was able to produce cooling from an average 37 and 39 °C to approximately 30 °C for the 1 and 2 mm wide channels of Diamond 1 and 2, respectively.

2.2. Analytic steady-state heat transfer model

To complement our experimental results, we developed an analytic steady-state heat transfer model to estimate the performance of a microfluidic thermally-controlled window and its dependence on scale, flow rates, water temperature, and material properties. When sunlight shines on the glass window, visible light passes through, but because the glass is effectively opaque to IR, radiative heating increases the temperature of the glass (Fig. 4). Heat diffuses through the glass, water-filled channel, and PDMS layers, while some energy is released back to the exterior and interior either as radiation or via air convection. Thus, when the exterior surface of the glass window is exposed to sunlight or heat, running cool water through the channels causes some of the energy to be absorbed and transported away, which prevents it from entering the room interior.

The steady-state analytic model was derived by an energy conservation argument that accounted for the thermal energy fluxes through the multiple layers of the window (glass, PDMS, water) and the thermal energy exchange with the exterior and interior air (for details, see SI). The model variables are the average cooling fluid temperature in the channel and the temperature along the exterior and interior sides of the window. The independent variable is the spatial coordinate in the direction of flow. Standard results from heat transfer [18] and fluid mechanics [19] were coupled with simplifying assumptions exploiting the following differences in length scales: the characteristic distances along the channel were much larger than the channel height and width; and the channel height was much smaller than the channel width and overall PDMS layer thickness. The steady-state model was developed in two steps. First, the preceding energy conservation argument was applied to the thermal fluxes across an infinitely wide window consisting of infinitely wide layers of glass and PDMS bounding an infinitely wide layer of water (Figs. 4,S1,S2). Second, the heat transfer across a finite window with evenly-distributed parallel channels was approximated by spatially averaging across and between the channels and applying a slight generalization of the steady-state model. The steady-state temperature of the cooling fluid in the channel, $T(x)$, and the steady-state temperature along the interior side of the window, $T_{IN}(x)$, both written in terms of the distance x along the channel from the inlet (for details, see SI), are

$$T(x) = T_\infty + (T_0 - T_\infty)\exp\left(-\frac{A\delta x}{Q}\right) \quad (1)$$

$$T_{IN}(x) = \frac{T(x) + B_p T_{room}}{1 + B_p} \quad (2)$$

where δ is the channel spacing (also defined for our diamond networks in Fig. S3), T_0 is the temperature of the water at the inlet, T_∞ is the static water temperature (i.e. when flow is off), T_{room} is RT, $B_p = 0.13$ is the Biot number characterizing the heat transfer through the PDMS layer, and A is a dimensional coefficient depending on the thermal properties of the PDMS, glass, and water. For water at 20 °C, $A = 1.94 \times 10^{-6}$ m/s (for details, see SI).

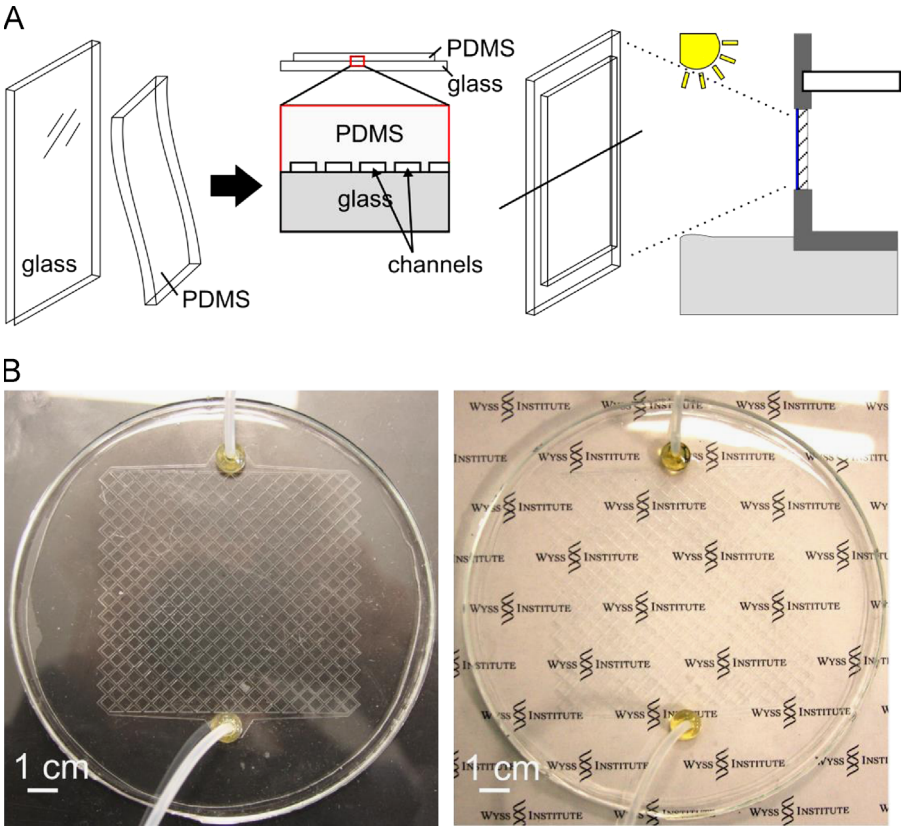

Fig. 1. Composite window with artificial vasculature. (A) Schematic of the composite window structure. (B) Diamond 1 PDMS layer having a 10×10 cm^2 array of 1 mm wide channels, dry (left) and filled with water (right).

For simplicity, we assume A is constant over the range of temperatures in the regime of interest (0–40 °C).

The predicted steady-state temperature profiles $T_{IN}(x)$ are compared to experimental measurements along the window centerline between the inlet and outlet of the diamond channel networks in Fig. 5. The spacing δ was calculated for our diamond networks (see Fig. S3 in the SI) as $\delta = 5.87$ mm and 11.9 mm for Diamond 1 and 2, respectively. In addition, since the channels zigzag across the window, the distance along the window equals the axial channel distance x divided by $2^{1/2}$. In the experiments, the inlet temperature was measured in the water bath at approximately 21 °C (RT). Tubing transported the water to the channels on the window. Pre-heating is evident from the data (Figs. 2, 5), since the window temperatures near the inlet were measured at 24–35 °C, warmer than the RT water bath. Thus, the measured inlet temperatures T_0 were used in the model. For the flow rates Q_w of 10, 2, 0.2 mL/min, $T_0 = 25.7$, 27.5 and 33.3 °C for Diamond 1 and $T_0 = 25$, 27.5 and 36.6 °C for Diamond 2, respectively. The static temperatures were measured for each of the flow rates 10, 2, 0.2 mL/min as $T_{IN\infty} = 37.7$, 36.5, and 36.6 °C for Diamond 1 and $T_{IN\infty} = 39.1$, 38.5, and 38.7 °C for Diamond 2, respectively. Note that the total flow rate Q_w was not split evenly between the channels in our diamond networks. In the SI, we calculate the flow along each segment of the diamond channel network using the analogy with electric circuits [20,21]; the average flow rates Q along segments parallel to the window centerline were $0.205Q_w$ and $0.281Q_w$ for Diamond 1 and 2, respectively. Substituting the above parameters into Eqs. (1) and (2) yields the predicted average window temperature as a function of distance across the window (Fig. 5). The agreement between experimental and simulation data is encouraging despite the simplifying assumptions made in the derivation. A straightforward improvement to the model would use the flow along each segment to predict the corresponding temperature profile along that segment. While finite element simulations could provide better estimates of both the steady state and transient window temperature, the main purpose of the model developed here was to make overall estimates of the proposed window cooling method.

2.3. Scaling up: cooling of full size (meter scale) windows

Vasculature systems are effective at both large and small scales, which we demonstrate by scaling up our estimates to full size (meter scale) windows. For the sake of making estimates, we apply our steady-state model to the simpler case of N parallel channels each separated by $\delta = W/N$ and distributed across a window of length L and width W. A total flow rate Q_w is delivered to the window, and a flow rate of $Q = Q_w/N$ is delivered to each channel. Combining (1) and (2), setting $x = L$, and solving for $Q_w = NQ$ relates the total flow rate Q_w to the temperature change (from $T_{IN}(0)$ to $T_{IN}(L)$) across the inner side of the window

$$Q_w = AWL\left|\ln\frac{T_{IN\infty} - T_{IN}(L)}{T_{IN\infty} - T_{IN}(0)}\right|^{-1} \tag{3}$$

Eq. (3) shows that the flow rate to cool the window scales as the window area LW, as expected from intuition. Thus, to scale up the flow rate of 2 mL/min used in our laboratory scale windows (0.1×0.1 m^2) to a full size 1.5×1.5 m^2 window, we would need a flow rate of $(1.5/0.1)^2 \times 2$ mL/min $= 450$ mL/min. However, as we show next, a lower flow rate can achieve the same level of cooling provided the inlet fluid is not preheated, as observed in our laboratory experiments. Another important property of Eq. (3) is that it is independent of the channel width, height, and spacing, even though these parameters affect the amount of pressure required to move fluid through the channels.

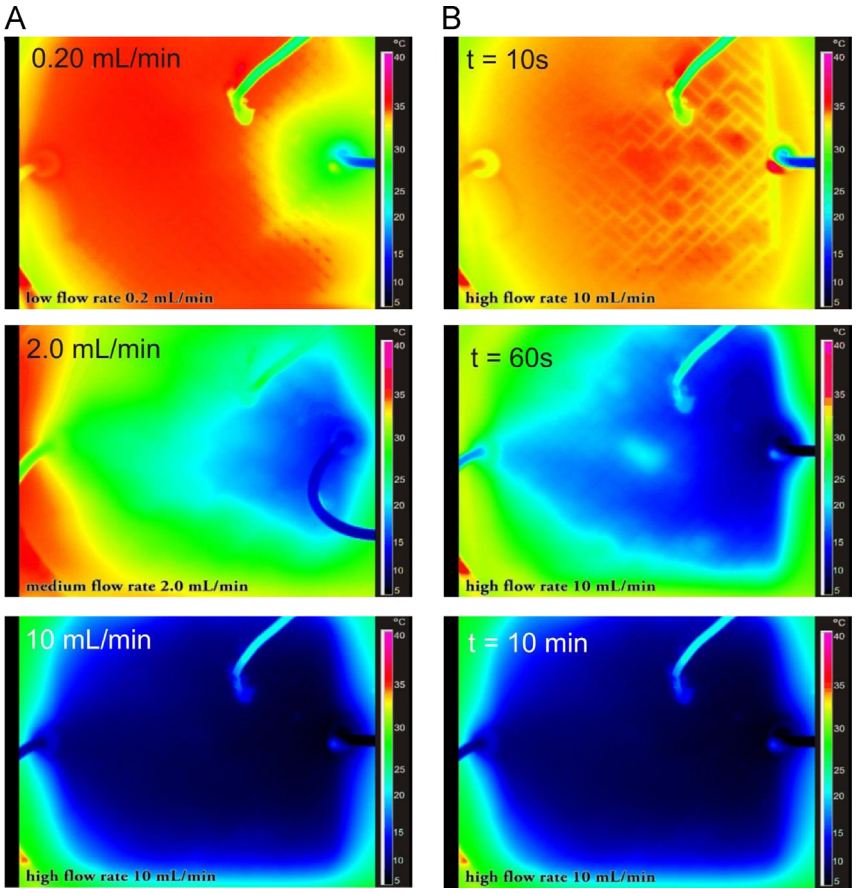

Fig. 2. Thermal IR images of the Diamond 1 PDMS channel layer for input water temperature of 0 °C. (A) Effect of flow rate, at steady state and (B) effect of time, at high flow rate (10 mL/min). In all images, inlet on right and output on left, flow is from right to left.

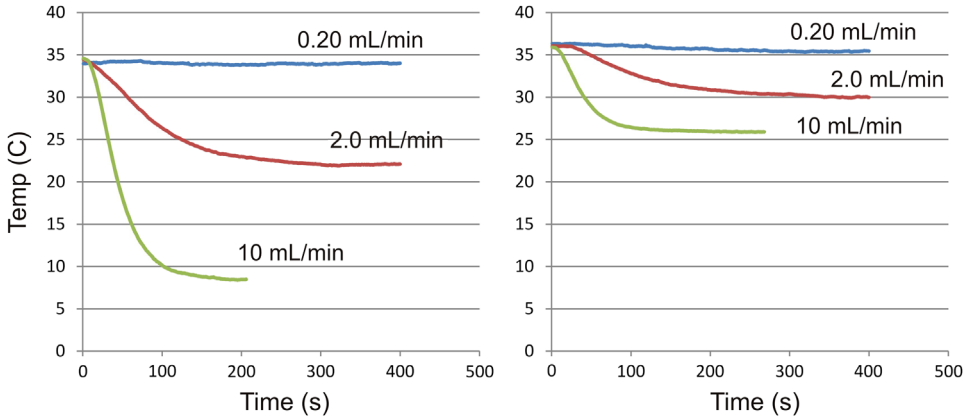

Fig. 3. Average window temperatures (averaged across a line between inlet and outlet, Diamond 1) as a function of time for input water temperatures of 0 °C (left) and room temperature (right).

To achieve a similar level of cooling (by ~10 °C) as in our laboratory experiments, we assume a static window temperature of $T_{IN\infty}=38$ °C, a final average inner window temperature of 28 °C, and inlet water and room temperatures of 21 °C. Thus, since the window temperature at $x=0$ is $T_{IN}(0)=21$ °C (same as inlet fluid and room temperature), we must keep the window temperature at $x=L$ at $T_{IN}(L)=35$ °C so that the average is 28 °C. Substituting these values into Eq. (3) yields the required net flow across the window channel network,

$$Q_w = 67\,LW \text{ mL/min} \quad (4)$$

where L and W are measured in m. For a full size window with $L=W=1.5$ m, we require a net flow of $Q_w=151$ mL/min to maintain the window temperature within the desired range.

One practical consideration when scaling up to full size windows is thermal expansion. Large windows exposed to sunlight may expand, contract, bend, and develop thermal gradients. Fortunately, the elasticity of PDMS should easily accommodate the deformation due to thermal strain, which is on the order of 50–90 μm per meter of window per °C for glass. At the scale of the channels, this is 0.05–0.09 μm per mm, negligible compared to the dimensions of the channels.

2.4. Estimates of pumping energies and gravity driven flows

We envision that the fluid can be fed and perfused through the channels in the PDMS layer using gravity, capillary action or an active pressure source, such as a pump or an elevated reservoir. For example, if fluid was fed into the top of the window (e.g., from a roof reservoir), gravity would be sufficient to drive fluid flow through the channels in the PDMS layer towards some cooling heat exchanger (e.g., placed in the ground), before being recirculated by a pumping mechanism. If the flow is gravity fed through N vertical, parallel, equispaced microchannels, resistance theory relates the flow rate $Q=Q_w/N$ through each channel to the hydrostatic pressure gradient $\Delta p=\rho gL$ along the channel and the channel resistance $R=12\,\mu L/(wh^3)$ (wide channel approximation, h/w small) as $\Delta p=RQ$ [20,21]. Solving for Q gives

$$Q=\frac{\rho g w h^3}{12\mu} \tag{5}$$

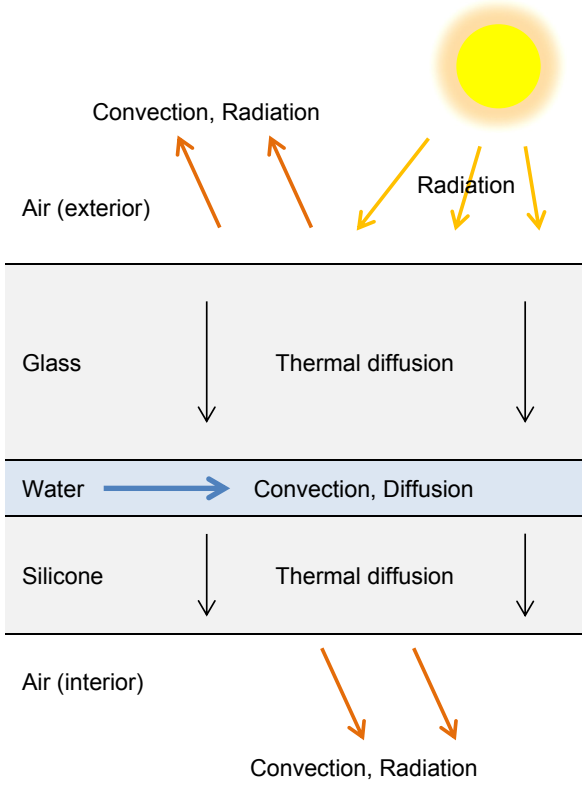

Fig. 4. Schematic of the heat transfer across a window with a composite system of glass and silicone microchannels containing flowing water.

Substituting Eq. (5) into Eq. (4), inserting the values for water, and solving for h gives

$$h=0.111(\alpha L)^{1/3}\ \text{mm} \tag{6}$$

where L is measured in m, $\alpha=\delta/w$ is the channel spacing to width ratio, and $\delta=W/N$. The main design criteria for gravity fed windows comes from Eq. (6), which relates the channel spacing, width, and height and the window length required to maintain a window at the conditions above, which include the flow rate (Eq. (4)) and temperature difference. For the sake of making estimates, we consider a window height of $L=1.5$ m. The fact that channels must be spaced more than their width apart is expressed by the constraint $\alpha>1$. Thus for meter scale windows ($L\sim1$ m), the channels would be on the 100 micron scale, similar to the microchannels used in our experiments. Moreover, adjustments to the channel spacing and width, parameterized via α, would make little difference to the required channel height due to the exponent ⅓ in Eq. (6). A relatively small channel spacing, say $\alpha=2$, requires a channel height $h=0.160$ mm, while a relatively large spacing $\alpha=10$ requires $h=0.274$ mm.

The energy required to pump water in this continuous flow cycle is actually quite small relative to the thermal energy that could be absorbed from the windows. For example, the energy required to raise 1 kg of water by a height of 2 m (e.g., to a 1st story window in a building) equals mass × gravity × height or 20 J (1 kg × 9.8 N/kg × 2 m). If that 1 kg of water is allowed to flow down (by gravity) through the channels of the window at a rate of 500 mL/min (taking 2 min), the power required to maintain the flow is 20 J/2 min=0.17 W, which is relatively low. Conversely, when that 1 kg of water, with a specific heat capacity of 4.19 J/gK, is heated by ~10 °C (i.e.; drawing heat from the window), it would absorb 4.19 J/gK × 1 kg × 10 °C=42 kJ of thermal energy. Assuming that power is directly related to the work done by an air-conditioning system, it represents a maximum theoretical power saving of 42 kJ/2 min=350 W. Thus, because of the high heat capacity of water, there is much more energy absorbed (42 kJ) due to the thermal 'role' of the water compared to the energy needed to pump it (20 J), and this scales directly with the power savings by the air-conditioning system cooling the building.

Lastly, if gravity feeding is not an option, such as for horizontal roof glazing or skylights, energy is needed to pump fluid across the window. The power I required to pump fluid through a channel at flow rate Q is $I=RQ^2$, where R is the channel resistance. For the sake of the calculation, we use the wide channel approximation listed above as $R=12\,\mu L/(wh^3)$. Thus, the power required to pump fluid across an entire window with N equispaced channels is $I_w=NRQ^2=RQ_w{}^2/N=12\,\mu\alpha LQ_w{}^2/(Wh^3)$. For example, we calculated above that cooling a 1.5 m × 1.5 m window by ~10 °C requires a

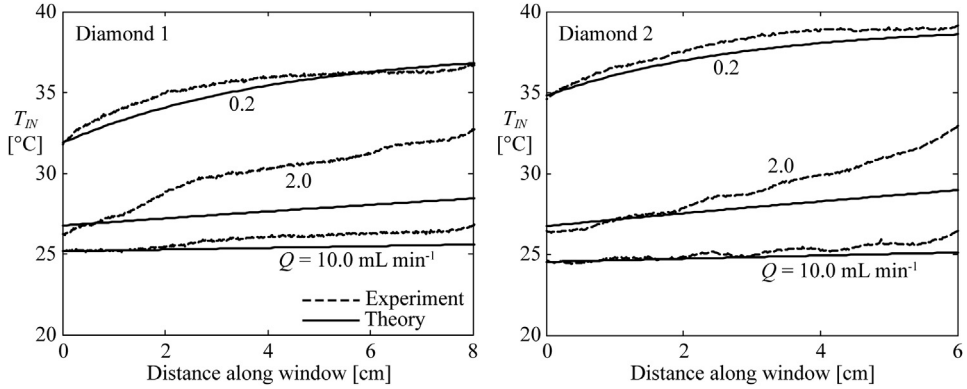

Fig. 5. Model predictions and experimental results for the average temperature T_{IN} across the interior side of the window, from inlet to outlet. The theoretical (Eq. (2)) and experimentally measured values of T_{IN} are plotted for three flow rates 0.20, 2.0 and 10 mL/min, for the Diamond 1 (left) and Diamond 2 (right) channel layers. Values of the inlet temperature T_0 and static temperature $T_{IN\infty}$ used in the model were obtained from measurements and are listed in the text.

total flow rate $Q_w = 151$ mL/min. The pumping energy required to maintain this flow rate across this window size is 0.019 W for channels of height $h = 200$ μm, closely spaced, $\alpha = 2$. Since the window cooling only depends on the temperatures, window size, and flow rate, and not directly on the width, height, and spacing of the channels (see Eq. (3)), these channel properties may be altered to lower the pumping power. In particular, the channels may be closely spaced (larger N, lower α) and be made thicker (larger h).

2.5. Controlling optical transparency

For many architectural applications, it is valuable to control window transparency or color, in addition to convective cooling. For this purpose, optically-absorbing dyes or cloudy (scattering) particle suspensions can be used. To explore this further, an aqueous suspension of carbon black was flowed into the Diamond 1 and 2 channel layers, gradually reducing the light transmissivity of the channel networks and making them significantly darker (Fig. 6 top and middle, respectively). Similarly, the color of the Diamond 2 channel network progressively changed from yellow to blue when water with common food dyes was infused through the microvascular network (Fig. 6, bottom).

To assess the effect of the microvascular layer on window transparency, we measured the optical transmission spectra (400–800 nm range). The measurements were normalized with respect to the optical transmission in air (value of 1.0) (Fig. 7). The glass window itself had a transparency value of about 0.9 over this spectral range. When overlaid with a PDMS layer containing empty microchannels, the transparency dropped to ~0.75 at 600 nm. When the channels were filled with water, the transparency increased slightly to ~0.8 at 600 nm. When filled with a cloudy suspension of TiO_2 nanoparticles (Sigma Aldrich), the transparency dropped to ~0.7 at 600 nm due to diffusive scattering, but dropped even further at shorter wavelengths (due to increased scattering; Fig. 7). Finally, when filled with the graphitic carbon suspension (Figs. 6,7), the transparency dropped to ~0.4 across the whole spectral range, and when flushed with water, the original transparency values were restored. Thus, window transparency can be actively tuned or adjusted over a range of transparencies by controlling the flow rate through the bio-inspired microvasculature.

3. Discussion

We have engineered a transparent microfluidic, thermal control, material coating layer for architectural windows that can provide

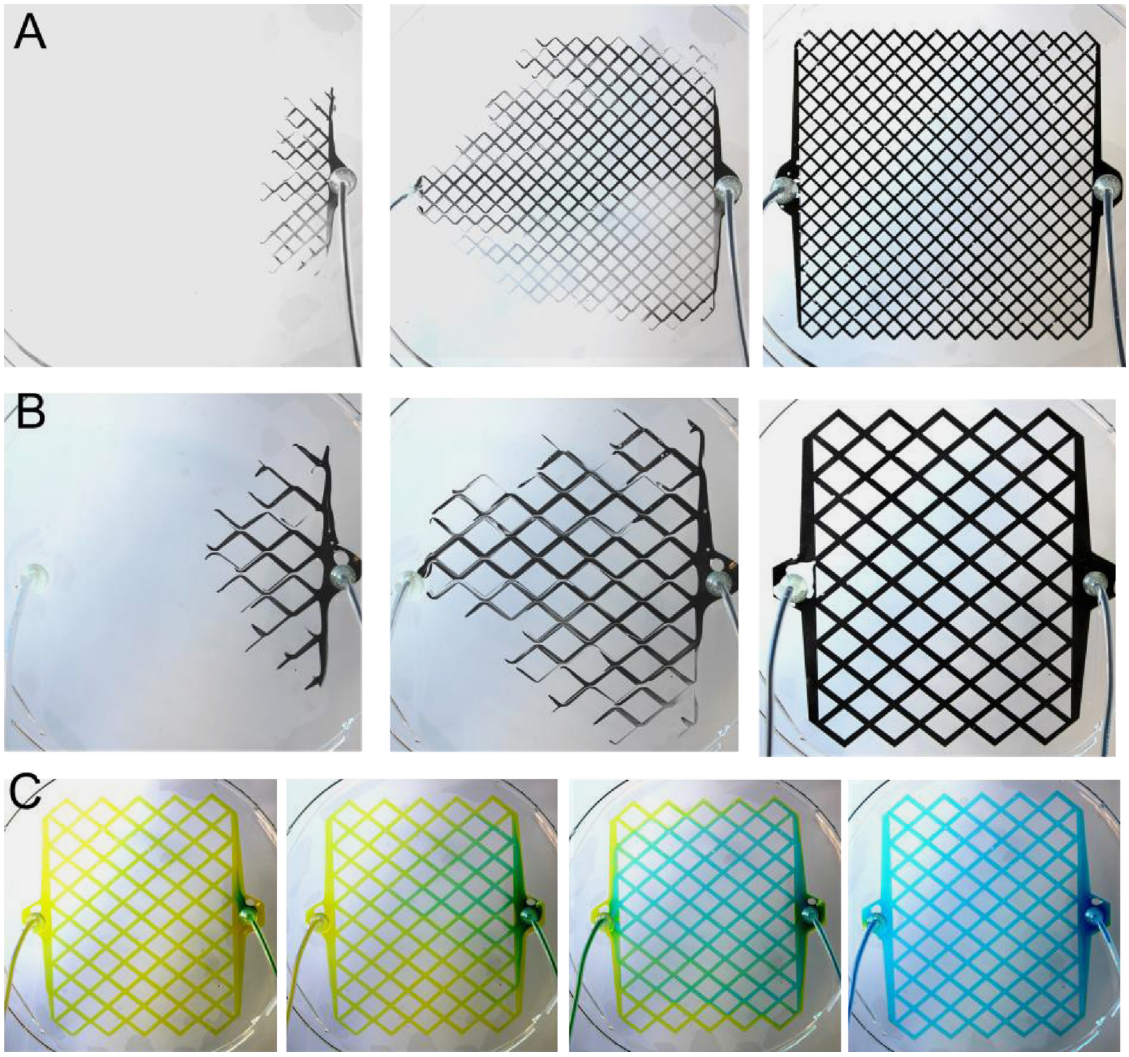

Fig. 6. Color change in microfluidic window layers: (A) Diamond 1, (B) Diamond 2 with graphitic carbon suspension flow and (C) Diamond 2 showing progressive color change using yellow and blue aqueous dye solutions. (For interpretation of the references to color in this figure legend, the reader is referred to the web version of this article.)

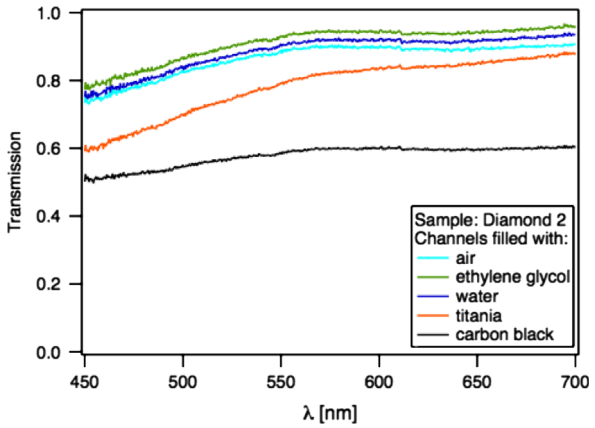

Fig. 7. Optical transmission spectra for the Diamond 2 channel layer as a function of fluid composition.

adaptive cooling and shading for buildings or photovoltaic applications. The thin cooling layer may be applied to one or more panes in multi-pane windows or as a thin non-structural central layer. The use of highly-transparent elastomer materials, such as silicone (PDMS), ensures that such windows still allow full transmission of visible light, which is a major advantage over many other adaptive shading technologies (often expensive) that greatly limit overall window transparency. For our laboratory model 10×10 cm^2 windows, we have demonstrated approximately 7–9 °C of cooling using RT water flowing at modest flow rates (2 mL/min or approximately 3 drops/s, where each water drop is the capillary length, 2.7 mm, in diameter).

To complement our experiments and to make predictions for full size windows, we developed an approximate theoretical model of the heat transfer through the multiple layers of our composite microchannel-cooled windows. The model predicts that the flow rate required to cool a window is determined solely by the desired temperature range across the window, window dimensions, and thermal properties (see Eq. (3)). In particular, the required flow rate is proportional to the window area. This flow rate may be produced via a pump, or, with gravity feeding, by a particular channel geometry. If the conditions of our laboratory experiments were scaled up to a full size 1.5×1.5 m^2 window, we would need a RT flow rate of $(1.5/0.1)^2 \times 2$ mL/min $= 450$ mL/min. Without the preheating of inlet fluid observed in the experiments, this value drops to 151 mL/min to achieve ~ 10 °C of cooling (see Eq. (4)). Since this RT water can be recirculated (with some secondary heat exchange), we believe that our cooling method presents a significant degree of cooling with a reasonably modest amount of flow. This cooling effect could greatly decrease the energy required for air conditioning, and further work will be done to model this at a larger, building scale.

The thermal energy transferred to the fluid phase can also be used as part of a solar energy harvesting system to supply heated water to an existing hot water system, or to a heat storage system, similar to existing solar heating (or hybrid photovoltaic/thermal) systems. And, as we have demonstrated, changing the optical properties of the fluid itself can be used to alter the overall window transparency and optimize this solar collection process. In the future, we envision an array of parallel heat exchange layers at inner and outer window surfaces connected by channels with fluids flowing in opposite directions through a central insulating layer, so that heat is exchanged across the window to increase the insulating efficiency of the window as a whole. The efficiency is derived from the use of a counter current heat exchanger design that mimics designs utilized for similar thermal stabilization effects in living organisms [17].

Experimental Section

Polydimethylsiloxane (PDMS, Sylgard 184, Dow Corning) layers (5 mm thick) were molded on an original master template, fabricated by cutting a pattern in an adhesive plastic layer (Sign Warehouse, 0.10 mm thick) by scribe-cutting (Graphtec cutting plotter CE5000-60), and layered on a flat glass surface. Two channel arrays spread over 10×10 cm^2 window areas were designed with microchannels 0.10 mm high and 1 or 2 mm wide (Diamond 1 and 2, respectively). The PDMS layers were bonded to 1/8″ glass by first treating with a corona arc discharge system (ETP, BD-20), then holding at 70 °C overnight. A syringe pump (Harvard Apparatus, PhD Ultra) was used to control the water flow through the PDMS layers, and a 150 W incandescent light placed approximately 50 cm away was used to heat the surface of the windows externally to an initial temperature of 35 to 40 °C before cooling. Thermal infrared (IR) measurements were made using a FLIR (SC 5600) camera, and 4 K-type thermocouples were attached to the PDMS and glass surfaces to verify the temperature measurements. Optical absorption measurements were made using an Ocean Optics spectrometer (USB2000) and a white light source.

Acknowledgments

BDH, IW, and DEI planned the research. BDH and IW fabricated devices and performed the experiments. MK aided in optical transparency measurements. MJH developed the theoretical model. BDH, DEI, IW, JA, and MJH wrote the paper. All authors revised the document and agreed on its final contents. We also thank Shuyun Wu for his work in the early phase of this project.

Appendix A. Supporting information

Supplementary data associated with this article can be found in the online version at http://dx.doi.org/10.1016/j.solmat.2013.06.027.

References

[1] U.S. Department of Energy (Ed.), Buildings Energy Data Book, D&R International Ltd., Silver Spring, MD, USA, 2009.
[2] S.E. Selkowitz, Thermal performance of insulating window systems, in: Proceedings of the ASHRAE Annual Meeting, Detroit, MI, 1979.
[3] J.A. Clarke, M. Janak, P. Ruyssevelt, Assessing the overall performance of advanced glazing systems, Solar Energy 63 (1998) 231–241.
[4] R. Baetens, B.P. Jelle, A. Gustavsen, Properties, requirements and possibilities of smart windows for dynamic daylight and solar energy control in buildings: a state-of-the-art review, Solar Energy Materials and Solar Cells 94 (2010) 87–105.
[5] S.P. Corgnati, M. Perino, V. Serra, Experimental assessment of the performance of an active transparent façade during actual operating conditions, Solar Energy 81 (2007) 993–1013.
[6] J.L. Warner, Selecting windows for energy efficiency, Home Energy 12 (1995) 11–16.
[7] D.R. Rosseinsky, R.J. Mortimer, Electrochromic systems and the prospects for devices, Advanced Materials 13 (2001) 783–793.
[8] D.J. Gardiner, S.M. Morris, H.J. Coles, High-efficiency multistable switchable glazing using smectic A liquid crystals, Solar Energy Materials and Solar Cells 93 (2009) 301–306.
[9] D. Arasteh, H. Goudey, C. Kohler, Highly insulating glazing systems using non-structural center glazing layers, in: Proceedings of the Annual ASHRAE Meeting, Salt Lake City, UT, 2008.
[10] T.-T. Chow, C. Li, Z. Lin, Innovative solar windows for cooling-demand climate, Solar Energy Materials and Solar Cells 94 (2010) 212–220.
[11] T.-T. Chow, C. Li, Z. Lin, Thermal characteristics of water-flow double-pane window, International Journal of Thermal Sciences 50 (2011) 140–148.
[12] E. Radziemska, The effect of temperature on the power drop in crystalline silicon solar cells, Renewable Energy 28 (2003) 1–12.

[13] J.J. Wysocki, P. Rappaport, Effect of temperature on photovoltaic solar energy conversion, Journal of Applied Physics 31 (1960) 571–578.
[14] E. Skoplaki, J.A. Palyvos, On the temperature dependence of photovoltaic module electrical performance: a review of efficiency/power correlations, Solar Energy 83 (2009) 614–624.
[15] H.A. Zondag, D.W. de Vries, W.G.J. van Helden, R.J.C. van Zolingen, A.A. van Steenhoven, The thermal and electrical yield of a PV-thermal collector, Solar Energy 72 (2002) 113–128.
[16] J.S. Coventry, Performance of a concentrating photovoltaic/thermal solar collector, Solar Energy 78 (2005) 211–222.
[17] P.G.H. Frost, W.R. Siegfried, P.J. Greenwood, Arterio-venous heat exchange systems in the Jackass penguin *Spheniscus demersus*, Journal of Zoology 175 (1975) 231–241.
[18] J.H. Lienhard IV, J.H. Lienhard V, A Heat Transfer Textbook, 4th ed., Phlogiston Press, Cambridge, MA, 2011.
[19] D.J. Acheson, Elementary Fluid Dynamics, Oxford, New York, 1990.
[20] A. Ajdari, Steady flows in networks of microfluidic channels: building on the analogy with electrical circuits, Comptes Rendus Physique 5 (2004) 539–546.
[21] K.W. Oh, K. Lee, B. Ahn, E.P. Furlani, Design of pressure-driven microfluidic networks using electric circuit analogy, Lab on a Chip 12 (2012) 515–545.